AIP | Applied Physics Letters

Direct measurement of donor-like interface state density and energy distribution at insulator/AlGaN interface in metal/Al2O3/AlGaN/GaN by photocapacitance method

M. Matys, B. Adamowicz, Y. Hori, and T. Hashizume

Citation: Appl. Phys. Lett. **103**, 021603 (2013); doi: 10.1063/1.4813407
View online: http://dx.doi.org/10.1063/1.4813407
View Table of Contents: http://apl.aip.org/resource/1/APPLAB/v103/i2
Published by the AIP Publishing LLC.

Direct measurement of donor-like interface state density and energy distribution at insulator/AlGaN interface in metal/Al_2O_3/AlGaN/GaN by photocapacitance method

M. Matys,[1] B. Adamowicz,[1] Y. Hori,[2] and T. Hashizume[2]
[1]*Institute of Physics—Center for Science and Education, Silesian University of Technology, Krzywoustego 2, 44-100 Gliwice, Poland*
[2]*Research Center for Integrated Quantum Electronics, Hokkaido University, Kita-13 Nishi-8, Kita-ku, 060-8628 Sapporo, Japan*

(Received 4 April 2013; accepted 23 June 2013; published online 10 July 2013)

We determined the energy distribution of donor-like interface state density $D_{itD}(E)$ at the Al_2O_3/AlGaN interface in a metal/Al_2O_3/AlGaN/GaN heterostructure (MISH) capacitor. In this order, we developed a point-by-point graphical method based on the measurement and simulations of the MISH photocapacitance versus ultraviolet light intensity. We found a tail-like shaped $D_{itD}(E)$ strongly decreasing from the value of 5×10^{13} to 4×10^{12} eV^{-1} cm^{-2} in the energy range between 0.12 eV and 0.45 eV from the AlGaN valence band edge. © *2013 AIP Publishing LLC*.
[http://dx.doi.org/10.1063/1.4813407]

The impact of electronic states at the insulator/AlGaN interface on AlGaN/GaN based devices, e.g., metal/insulator/semiconductor heterostructure field effect transistors (MISHFETs) has been well established.[1] The interface states are responsible for natural formation of a two-dimensional electron gas (2DEG), at the AlGaN/GaN interface and, on the other hand, for such undesired effects as virtual-gate formation and drain current collapse.[2–7] In spite of that, the main issues regarding interface states, i.e., their nature and density distribution $D_{it}(E)$ in the most part of the AlGaN band gap is still under debate. In the literature, three main models of donor-like interface states were considered, namely a discrete level and states with uniform[2,8–10] or U-shaped density distribution[5] in the AlGaN band gap. It should be stressed that the standard electrical methods for determining $D_{it}(E)$, including capacitance- and conductance-based approaches are very difficult in the case of metal/insulator/AlGaN/GaN heterostructure (MISH) capacitors because of two interfaces and extremely long time constants for charge emission from the deep states at room temperature (RT).[11] Recently, from the capacitance-voltage (C–V) hysteresis and photo-assisted C–V the interface states $D_{it}(E)$ distributed around the AlGaN midgap and acceptor-like states near the conduction band edge (E_C) were reported.[12,13] However, the energy distribution of the donor interface state density at the AlGaN surface is completely unknown.

In this letter, we determined directly the donor-like interface state density distribution $D_{itD}(E)$ at the Al_2O_3/AlGaN interface in a metal/Al_2O_3/AlGaN/GaN MISH capacitor in the energy range between 0.12 eV and 0.45 eV from the valence band edge (E_V). In this order, we modified our method based on the measurement and simulations of the photocapacitance (C_L) versus excitation ultraviolet (UV) light intensity (Φ), which was recently developed by Matys *et al.*[14] for the determination of the donor-like interface states in Al_2O_3/GaN MIS. Here, from a graphical approach, we obtained $D_{itD}(E)$ in a point-by-point manner.

The investigated Al_2O_3 (20 nm)/$Al_{0.25}Ga_{0.75}N$ (30 nm)/GaN structure was intentionally undoped (electron concentration in AlGaN of 5×10^{15} cm^{-3}). The Ni/Au (20/50 nm) gate was circular, and Ti/Al/Ti/Au ohmic contact was ring shaped. The Al_2O_3 passivation layer was grown by atomic layer deposition at 350 °C. The scheme of the studied MISH capacitor structure and technological details are described in Ref. 13. The photocapacitance for the gate bias V_G from −4.0 to −2 V was measured at 1 MHz at RT. In addition, the surface photovoltage (SPV) at the Al_2O_3/AlGaN interface, i.e., the change in the contact potential difference upon illumination, was registered using the Besocke Kelvin probe. As a light source, a xenon lamp and a band-pass filter ($\lambda = 300$ nm) were applied. The exemplary C_L transients after switch on and off the light, for $V_G = -3$ V, are shown in Fig. 1(a). One can note that the steady-state C_L response for higher Φ was achieved after longer time. In the measurement of $C_L(\Phi)$ dependencies to assure the steady-state C_L, for all Φ we assumed a period of about 60 min, as for the largest Φ. After UV off a very slow decrease of the C_L signal was observed. This transient can be attributed to the long restoring of the potential barrier at the Al_2O_3/AlGaN interface, which was reduced under UV illumination. This effect is probably determined by the change in the interface charge due to slow capturing electrons emitted thermionically from 2DEG.[15] The time dependence of barrier recovery was proven from the SPV transient measured for non-biased structure (Fig. 1(b)). After 50 min of UV off (with different intensity) the C–V measurements were performed, first in the V_G range from −3 to −14 V, and then from −14 to 6 V. From Fig. 1(c), it results that the obtained C–V curves exhibit the parallel shift (larger after higher Φ) towards the negative voltage. This shift is due to a widening of the energy range of the interface states, which changes their total charge Q_{it} upon UV illumination and behave as a fixed charge after UV switch off. The dependence of C–V voltage shift (ΔV) versus Φ is shown in Fig. 1(d). We found

that this dependence is expressed by the relationship $\Delta V \sim \Phi^{0.042}$. The full structure reset was realized by applying a positive bias $V_G = 6\,\mathrm{V}$ necessary to attract electrons from the AlGaN/GaN interface to Al_2O_3/AlGaN interface, where they are captured by the interface states. It should be mentioned that the measured photo and dark leakage current was negligibly small (less than $20\,\mathrm{nA/cm^2}$) for the photocapacitance experiment.

Our method for the determination of the donor $D_{itD}(E)$ is based on the following model of non-equilibrium effects in an Al_2O_3/AlGaN/GaN MISH. The structure illuminated with photon energy above AlGaN band gap is biased with the negative V_G for which the corresponding total structure capacitance C_{dark} in the dark is equal to ${C_{dark}}^{-1} = {C_{AlGaN}}^{-1} + {C_{Al_2O_3}}^{-1}$, where C_{AlGaN} and $C_{Al_2O_3}$ is the capacitance of the AlGaN and Al_2O_3, respectively. On the other hand, V_G should be negative enough to quench the interface recombination at Al_2O_3/AlGaN, similarly to the case of Al_2O_3/GaN interface, as we proved in our previous work.[14] Under excitation the MISH total photocapacitance (C_L) changes with respect to the dark value (C_{dark}) due to C_{AlGaN} variations. This is because excess electrons and holes are separated in the electrical field in AlGaN (scheme in Fig. 2). The holes are attracted towards the Al_2O_3/AlGaN interface, whereas electrons are both repelled by the negative V_G and attracted by the positive fixed charge at the AlGaN/GaN interface. Furthermore, due to the positive valence band offset[16] (*VBO*) of Al_2O_3 with respect to AlGaN the flow of photoholes through dielectric film is impossible. The holes are captured by the donor-like interface states, which become positively ionized. On the contrary, the deep acceptor-like states, if exist, are not ionized due to lack of electrons at the interface but become neutralized due to hole capturing. Upon increasing Φ and rising number of excess holes, the hole quasi-Fermi level at the interface, E_{Fp}, scans the widening range of interface states distributed in the AlGaN band gap. In contrast, the electron quasi-Fermi level, E_{Fn}, is almost constant at the interface.

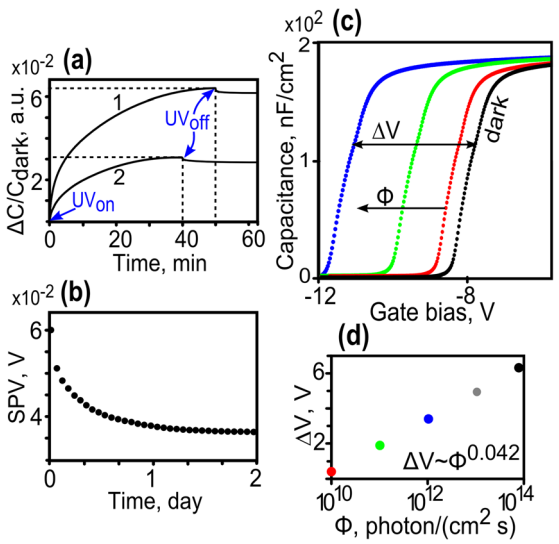

FIG. 1. Relative C_L transients of AlGaN MISH at RT for Φ_1 (curve 1) $> \Phi_2$ (curve 2) (a), SPV transient (b), C–V curves measured in the dark after illumination with increasing intensity Φ (c), and voltage shift of C–V curves versus Φ (d).

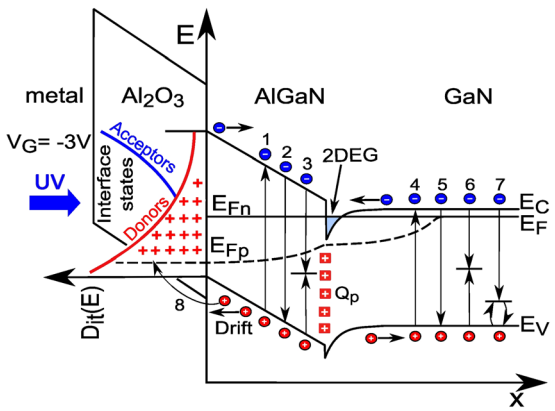

FIG. 2. Illuminated and negatively biased AlGaN/GaN MISH, (1, 4) electron-hole generation in AlGaN and GaN, respectively, (2, 5) band-to-band recombination, (3, 6) non-radiative bulk SRH recombination, (7) radiative point defect transitions, and (8) hole capturing by interface states.

For the calculation of the Al_2O_3/AlGaN/GaN MISH photocapacitance, we used one-dimensional drift-diffusion model.[17] We assumed that the generation rate decreases exponentially versus the distance from the interface with different absorption coefficients in AlGaN and GaN layers. We took into account all main bulk recombination channels, i.e., radiative band-to-band recombination, non-radiative Shockley-Read-Hall (SRH) recombination, transitions through deep acceptor levels in GaN (related to so-called yellow photoluminescence, PL) and also interface recombination through the interface states distributed at the Al_2O_3/AlGaN interface, in terms of the SRH statistics as described in Ref. 14. The AlGaN and GaN bulk parameters for these calculations were taken from Ref. 1 and parameters used in the relationships describing yellow PL in GaN from Ref. 18. We assumed different donor $D_{itD}(E)$ and acceptor-like $D_{itA}(E)$ interface state density distributions in the whole AlGaN bandgap at the Al_2O_3/AlGaN interface and neglected the states at AlGaN/GaN one. In addition, the net interface fixed charge Q_{net} at the Al_2O_3/AlGaN interface (polarization charge and ionized defects) and the fixed polarization charge ($Q_p = 1.2 \times 10^{13}\,\mathrm{q\,cm^{-2}}$)[1] where q is the elementary charge) at the AlGaN/GaN interface were taken into account.

The sheet density of the total charge (Q_{it}) at the Al_2O_3/AlGaN interface is described by the following formula:

$$Q_{it} = Q_{itD} + Q_{itA} = \int_{E_V}^{E_C} D_{itD}(E)(1 - f_{it})q\,dE - \int_{E_V}^{E_C} D_{itA}(E) f_{it} q\,dE, \quad (1)$$

where Q_{itD} is the donor-like state charge and Q_{itA} is the acceptor-like state charge; f_{it} is the occupation function taken from Ref. 14.

At the Al_2O_3/AlGaN and AlGaN/GaN interfaces, we used the Neumann boundary conditions. Namely, at the Al_2O_3/AlGaN interface

$$\epsilon_{Al}\epsilon_0 E_{Al} - \epsilon_I \epsilon_0 E_I = Q_{it} + Q_{net}, \quad (2)$$

where $\epsilon_{Al,I}$ is the AlGaN and Al_2O_3 dielectric constant, respectively, ϵ_0 is the vacuum permittivity, $E_{Al,I}$ is the electric field intensity in AlGaN and insulator, respectively.

Boundary conditions at the contacts are the Dirichlet type, i.e., at the gate (x = 0) $V = V_G - \phi_s/q + \phi_b/q$, where V_G is the gate voltage, ϕ_s is the surface barrier height (for Ni/Al_2O_3, $\phi_s = 3.5$ eV), and ϕ_b is the built-in potential (in eV), respectively, and $V = 0$ at the Ohmic contact. The boundary conditions for the continuity equations are given in terms of the interface recombination rate. In the C_L calculation, like in Ref. 14, we assumed that the interface state charge cannot follow the fast AC voltage signal (h-f measurement). The model equations were solved self-consistently using a finite element method with the very good convergence (relative error at the level of 10^{-6}) to obtain the in-depth distribution of electric potential and carrier densities in MISH.

In order to determine $D_{itD}(E)$ at the Al_2O_3/AlGaN interface, the analysis of Al_2O_3/AlGaN/GaN MISH photocapacitance C_L and main Al_2O_3/AlGaN interface electronic parameters versus Φ, i.e., E_{Fp}, excess hole concentration p_s, and Q_{itD} was performed. In the analysis, we neglected $D_{itA}(E)$ because they do not influence the C_L response as it will be proven in the experimental result discussion. The results of calculations for the structure biased with $V_G = -3\,V$ and various $D_{itD}(E)$ distributions (flat and exponential) in the AlGaN band gap are shown in Figs. 3(a)–3(e). From Fig. 3(a), it is evident that a given C_L value (in terms of $\Delta C = C_L - C_{dark}$) can be reproduced by means of different $D_{itD}(E)$ distributions (point A in Fig. 3(a)). It results from the fact that for all relevant $D_{itD}(E)$, the total number of holes captured by donor-like states for a given Φ (corresponding to point A), and thus, the actual interface E_{Fp} position in the AlGaN band gap must be the same. This is supported by the calculations, which give the same value of p_s and Q_{itD} at point A for the different $D_{itD}(E)$ as shown in Figs. 3(b) and 3(c). All these prove that for an exemplary $C_L(\Phi)$ curve calculated for an exponential $D_{itD}(E)$ function, we can find a set of the equivalent flat $D_{itD}(E)$ distributions as well as corresponding Q_{itD}, p_s, and, thus, E_{Fp}. Therefore, the average local value of $D_{itD}(E)$ can be found from the relationship:

$$D_{itD}(E) = \left| \frac{{Q_{itD}}^C - {Q_{itD}}^B}{{E_{Fp}}^C - {E_{Fp}}^B} \right|, \quad (3)$$

where $Q_{itD}^{B,C}$ and $E_{Fp}^{B,C}$ are the values of interface donor charge and hole quasi-Fermi level corresponding to points B and C, respectively. On the basis of the above approach, we reproduced very well in point-by-point manner the assumed exponential curve $D_{itD}(E)$ (dots on the reproduced curve 1 in Fig. 3(d)). From Fig. 3(c), it results that the $Q_{itD}(\Phi)$ curves exhibit different slopes depending on the $D_{itD}(E)$ shape, i.e., the slope is larger for stronger $D_{itD}(E)$ increasing towards E_V. In particular, $Q_{itD} \sim \Phi^{0.015}$ for all flat state density distributions. We also proved that the determined $D_{itD}(E)$ does not depend on both the net interface fixed charge Q_{net} and excess carrier lifetime τ. In this order, we analyzed $Q_{itD}(E_{Fp})$ dependencies (shown in Fig. 3(e)), which were obtained using the above

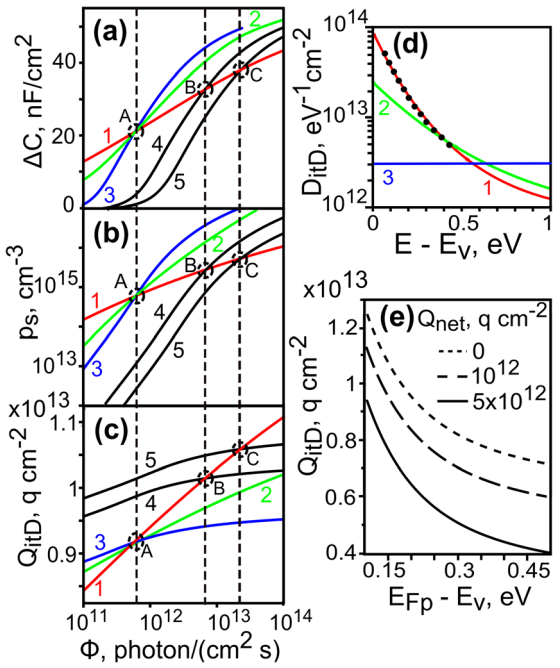

FIG. 3. Calculated photocapacitance with respect to the dark value $\Delta C = C_L$-C_{dark} of AlGaN MISH vs. Φ (a), and corresponding dependencies of $p_s(\Phi)$ (b) and $Q_{itD}(\Phi)$ (c) for different $D_{itD}(E)$ curves 1–3 (d); curves 4 and 5—for flat $D_{itD}(E)$ not shown here; dots on curve 1 of $D_{itD}(E)$ mean values obtained by the described method; $Q_{itD}(E_{Fp})$ also obtained by this method from curve 1 of $\Delta C_L(\phi)$ for different Q_{net}(e).

method for curve 1 in Fig. 3(a), assuming different Q_{net}. The calculation was performed for the positive Q_{net} taken from the literature.[19,20] From Fig. 3(e), it results that Q_{net} causes a parallel shift of $Q_{itD}(E_{Fp})$ curves with respect to an Q_{itD} axis without changing their slope. For larger Q_{net}, the interface charge Q_{itD} was lower because of the reduced number of holes at the Al_2O_3/AlGaN interface due to their repelling by Q_{net}. Thus, the actual $D_{itD}(E)$ value (from Eq. (2)) is the same for various Q_{net}. Analogously τ influences the determined Q_{itD}, as it was proven from the simulations carried out for different $\tau = 10^{-7}$ and 10^{-9} s. This is due to the constant quantum efficiency of the bulk SRH recombination rate in the analyzed Φ range because of the negligible interface recombination.

Subsequently, we analyzed the experimental $C_L(\Phi)$ dependencies upon UV excitation in order to determine $D_{itD}(E)$ at the Al_2O_3/AlGaN interface. It should be noted that these dependencies were measured for different V_G to extend the energy range of scanned interface states by shifting E_F. At first, we excluded the possible contribution of the $D_{itA}(E)$ to $C_L(\Phi)$ dependencies from the comparison of the experimental and simulated curves, as summarized in Fig. 4. It is evident that the $C_L(\Phi)$ curve 1 corresponding to $D_{itA}(E)$ ($Q_{it} < 0$) is shifted toward lower Φ values with respect to the ideal curve. In contrary, curve 3 corresponding to $D_{itD}(E)$ ($Q_{it} > 0$) is shifted toward higher Φ, the same like the experimental $C_L(\Phi)$ curves (points), which are shifted even more by several orders of magnitude. One can also note that the shift of experimental curves is much larger than the shift due to the positive Q_{net}. On this basis, we concluded that mainly $D_{itD}(E)$ are responsible for the experimental $C_L(\Phi)$ responses. Then, we generated a set of $C_L(\Phi)$ curves corresponding to flat $D_{itD}(E)$

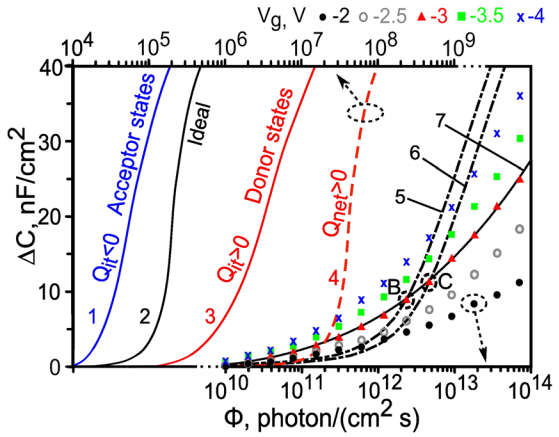

FIG. 4. Calculated (solid lines) and measured (points) ΔC vs. Φ for Al_2O_3/AlGaN/GaN MIS-H; curves 1 and 3 are for acceptor and donor states, respectively; curve 2 is for $D_{itD}(E) = D_{itA}(E) = 0$; curve 4 is for $Q_{net} = 5 \times 10^{12}\,\mathrm{q\,cm^{-2}}$ without interface states; curves 1–4 are for $V_G = -3\,\mathrm{V}$; curves 5 and 6 correspond to flat $D_{itD}(E)$ passing through chosen points B and C, and best-fit curve 7 for exponential $D_{itD}(E)$ shown in Fig. 5.

distributions, which pass through all experimental points, as shown in Fig. 4, and calculated $D_{itD}(E)$ from Eq. (2). Additionally, from the measured $C_L(\Phi)$ curves the $Q_{itD}(\Phi)$ dependencies for different Q_{net} were determined and summarized in the inset in Fig. 5. One can note that the experimental $Q_{itD}(\Phi)$ (despite of Q_{net}) and $\Delta V(\Phi)$ curves are the same functions on Φ. This correlation is an additional support of the donor character of the observed interface states. The obtained $D_{itD}(E)$ distribution at the examined Al_2O_3/AlGaN interface is presented in Fig. 5. One can note that the parts of $D_{itD}(E)$ curves for different V_G (points) are overlapping. The $D_{itD}(E)$ value reaches $5 \times 10^{13}\,\mathrm{eV^{-1}\,cm^{-2}}$ at 0.12 eV above E_V and strongly decreases to $4 \times 10^{12}\,\mathrm{eV^{-1}\,cm^{-2}}$ around the 0.45 eV level. The experimental points are approximated by the exponential function corresponding to the continuous $D_{itD}(E)$ (solid line). The theoretical dependence $C_L(\Phi)$ calculated for this function and $V_G = -3\,\mathrm{V}$ fits very well to the experimental one, as shown in Fig. 4. It is interesting to point out that the similar decaying $D_{itD}(E)$ was found for Al_2O_3/GaN MIS.[14] The obtained $D_{itD}(E)$ distribution for the passivated AlGaN interface resembles a band-tail exponential interface state continuum, which was postulated within the unified model for electronic states at free surfaces and Schottky interfaces[5] of AlGaN. According to this model, such continuous states in the AlGaN bandgap result from the interfacial disorder of bond lengths and angles.

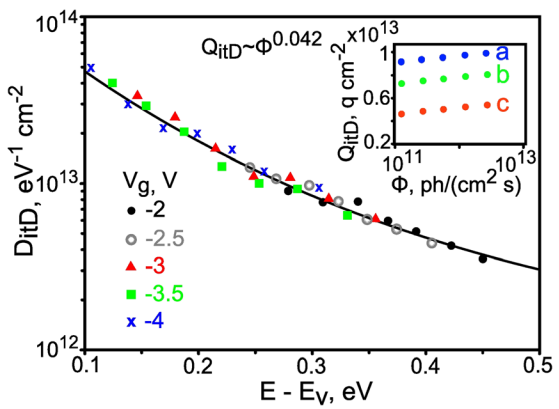

FIG. 5. Determined $D_{itD}(E)$ at Al_2O_3/AlGaN interface; in the inset corresponding $Q_{itD}(\Phi)$ for different $Q_{net} = 0$ (a), $1 \times 10^{12}\,\mathrm{q\,cm^{-2}}$ (b), $5 \times 10^{12}\,\mathrm{q\,cm^{-2}}$ (c).

It should be noted that the presented method for determining $D_{itD}(E)$ requires high-k insulating layers with positive *VBO* and negligible leakage currents. However, it can be also implemented for ultrathin dielectric layers after taking into account a photo-hole tunneling. The case for dielectrics with negative *VBO* will be analysed in our future work.

In conclusion, we determined quantitatively in a point-by-point manner the donor-like interface state density distribution $D_{itD}(E)$ at the Al_2O_3/AlGaN interface which was impossible to achieve by other methods. In the near E_V region, the shape of $D_{itD}(E)$ resembles a tail extending into the valence band. It should be stressed that the obtained result is crucial to understand the main electronic properties of both AlGaN/GaN MIS structures and free AlGaN surfaces as well as interface state origin. The method reported here can be easily applied for heterostructures of various wide band gap semiconductors. We thank R. Ucka, M.Sc. Eng., for his help in experiment.

The work was partially supported within InTechFun project (UDA-POIG.01.03.01.00-159/08-04) of EU Structural Funds in Poland.

[1]H. Morkoc, *Handbook on Nitride Semiconductors and Devices, GaN-Based Optical and Electronic Devices* (Wiley, Weinheim, 2009), Vol. 3.
[2]J. P. Ibbetson, P. T. Fini, K. D. Ness, S. P. DenBaars, J. S. Speck, and U. K. Mishra, Appl. Phys. Lett. **77**, 250 (2000).
[3]B. Jogai, J. Appl. Phys. **93**, 1631 (2003).
[4]I. P. Smorchkova, C. R. Elsass, J. P. Ibbetson, R. Vetury, B. Heying, P. Fini, E. Haus, S. P. DenBaars, J. S. Speck, and U. K. Mishra, J. Appl. Phys. **86**, 4520 (1999).
[5]H. Hasegawa, T. Inagaki, S. Ootomo, and T. Hashizume, J. Vac. Sci. Technol. B **21**, 1844 (2003).
[6]C. Roff, J. Benedikt, P. J. Tasker, D. J. Wallis, K. P. Hilton, J. O. Maclean, D. G. Hayes, M. J. Uren, and T. Martin, IEEE Trans. Electron Devices **56**, 13 (2009).
[7]R. Vetury, N. Q. Zhang, S. Keller, and U. K. Mishra, IEEE Trans. Electron Devices **48**, 560 (2001).
[8]G. Koley and M. G. Spencer, Appl. Phys. Lett. **86**, 042107 (2005).
[9]M. Higashiwaki, S. Chowdhury, M.-S. Miao, B. L. Swenson, C. G. Van de Walle, and U. K. Mishra, J. Appl. Phys. **108**, 063719 (2010).
[10]L. Gordon, M.-S. Miao, S. Chowdhury, M. Higashiwaki, U. K. Mishra, and C. G. Van de Walle, J. Phys. D: Appl. Phys. **43**, 505501 (2010).
[11]M. Miczek, C. Mizue, T. Hashizume, and B. Adamowicz, J. Appl. Phys. **103**, 104510 (2008).
[12]M. Fagerlind, F. Allerstam, E. O. Sveinbjornsson, N. Rorsman, A. Kakanakova-Georgieva, A. Lundskog, U. Forsberg, and E. Janzen, J. Appl. Phys. **108**, 014508 (2010).
[13]C. Mizue, Y. Hori, M. Miczek, and T. Hashizume, Jpn. J. Appl. Phys., Part 1 **50**, 021001 (2011).
[14]M. Matys, B. Adamowicz, and T. Hashizume, Appl. Phys. Lett. **101**, 231608 (2012).
[15]G. Koley, H.-Y. Cha, C. I. Thomas, and M. G. Spencer, Appl. Phys. Lett. **81**, 2282 (2002).
[16]T. Hashizume, S. Ootomo, and H. Hasegawa, Appl. Phys. Lett. **83**, 2952 (2003).
[17]S. Selberherr, *Analysis and Simulation of Semiconductor Devices* (Springer, Wien, 1984).
[18]M. A. Reshchikov and R. Y. Korotkov, Phys. Rev. B **64**, 115205 (2001).
[19]M. Esposto, S. Krishnamoorthy, D. N. Nath, S. Bajaj, T.-H. Huang, and S. Rajan, Appl. Phys. Lett. **99**, 133503 (2011).
[20]S. Ganguly, J. Verma, G. Li, T. Zimmermann, H. Xing, and D. Jena, Appl. Phys. Lett. **99**, 193504 (2011).